OXYGEN DIVACANCY MODEL FOR THE E'' CENTERS

IN CRYSTALLINE SiO_2

By .

BRIAN LEONARD MIHURA

Bachelor of Science in Arts and Sciences

Oklahoma State University
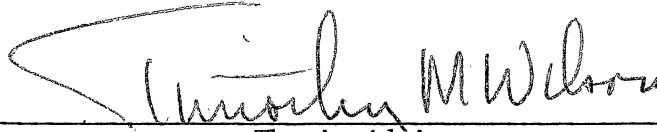
Stillwater, Oklahoma

1981

Submitted to the Faculty of the Graduate College
of the Oklahoma State University
in partial fulfillment of the requirements
for the Degree of
MASTER OF SCIENCE
July, 1984

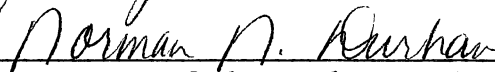OXYGEN DIVACANCY MODEL FOR THE E'' CENTERS

IN CRYSTALLINE SiO$_2$

Thesis Approved:

_____
Thesis Adviser

_____
Larry E. Halliburton

_____
Joel J. Martin

_____
Norman N. Durham
Dean of the Graduate College

ACKNOWLEDGMENTS

TABLE OF CONTENTS

LIST OF TABLES

LIST OF FIGURES

CHAPTER I

INTRODUCTION

Radiation-induced defects in quartz have been studied for the past thirty years. Of these defects, the spin $= \frac{1}{2}$ defects, i.e., the E_1', E_2', E_4' and the Al-hole centers, have been explored in detail due to their distinct ESR profile. Recently new research has been done on certain spin $= 1$ defects labeled by Halliburton et al., as E'' centers.

The earliest report of spin $= 1$ defects in quartz was made by Weeks and Abraham (1, 2) in 1964. In their work they tentatively concluded that this defect was not associated with any known impurity. They surmised that the spin $= 1$ state was due to a dipole-dipole interaction of two nearby electrons in spin $= \frac{1}{2}$ states and that these electrons were in incomplete next-nearest-neighbor silicon orbitals. Their study led them to state that the defect is a meta-stable one and is different from the E_1' center.

The topic was not addressed again until Solnstev, Mashkovtsev and Shcherbakov (3) published their paper in 1977. They suggested that the defect was due to a chain of vacancies with a coupled pair of electrons rising from silicon atoms roughly 6 $\overset{\circ}{A}$ apart. They also noted some correlation in the intensities of the E_1' and the spin $= 1$ defects. From this they drew the conclusion that the two defects were manifestations of the same many-vacancy defect in different charge states.

1

The most detailed and thorough study of the E" centers was made by Bossoli, Jani and Halliburton (4). The important points brought forth in their work were i) at least three separate E" centers existed, nomenclatured E_1'', E_2'' and E_3''; ii) the formation of the E" centers is a two-step process; iii) the E_2'' center anneals out near $50^{\circ}C$, while the more stable E_1'' and E_3'' anneal out near $85^{\circ}C$ and $95^{\circ}C$ respectively. It was then suggested that the E" defect was an oxygen divacancy which to the first approximation would be equivalent to two neighboring E_1' centers. The calculated separation between the two interacting silicons was approximately 5 $\overset{o}{A}$ for the E_1'' center, and larger values were estimated for the other two. It is on this model that the present study was based.

Computer modeling of quartz defects has proven to be both useful and accurate. The first of these studies was carried out by Yip and Fowler (5) on the E_1' center. Their model of the center consisted of an oxygen vacancy with an unpaired electron from the short-bonded silicon in that vacancy. Using a linear combination of localized orbitals-molecular orbital (LCLO-MO) cluster method on a CDC 6400 computer, they obtained reasonable results for the electronic energy levels. An analysis of the hyperfine tensor also showed broad agreement with experiment. As a result of their efforts, the model proposed in their study is the presently accepted description of the E_1' center.

Following on the success with the E_1' center, Isoya, Weil and Halliburton (6) performed computer modeling on the E_4' center. This model was essentially an E_1' with a hydride ion, rather than an electron trapped in the vacancy. The _ab_ _initio_ self consistent field-molecular orbital (SCF-MO) cluster program Gaussian 70 was employed in this project on a DEC 2050 computer and later on an IBM 370/158. Here, too, the agreement

between the calculations and experimental data was good, though only on a limited basis. In general, the results of the present calculations are supportive of the assumptions made in the model.

Most recently Mombourquette, Weil and Mezey (7) modeled AlO_4 centers in quartz on a DEC 2060 computer. For this study, Gaussian 70 and a version of the advanced Gaussian 76 program named Monstergauss was used. Once again the agreement between experimental and computational results was good. The calculated total energies, charge densities, spin densities and structural parameters were consistent with experiment. Insight on detailed orbital states was also made available.

The present study is an attempt to follow on these earlier successes with a viable model for the E'' centers. The program utilized is the latest of the Gaussian ab initio SCF-MO programs, Gaussian 80 and the computing device is the IBM 3081D. Electronic energy levels and electron orbital distributions will be examined, as will their charge distribution and spin densities. Total energies and relative energy minimizations will likewise be carried out to study relaxations of various atomic parameters. With sufficient agreement in these areas, the oxygen divacancy will be proposed as the source of at least one of the E'' centers.

CHAPTER II

PROCEDURE

In order to implement the Gaussian 80 program, a well defined cluster had to be constructed. The formation of the several clusters will be discussed, as will the means by which the program utilizes these clusters. A brief overview of the Gaussian 80 program will also be presented, as well as an outline of its application in this study and the difficulties encountered therein.

Cluster Construction

Quartz has a hexagonal unit cell with a crystallographic coordinate system comprised of two axes, $\vec{a}_1$ and $\vec{a}_2$, making an angle of 120° with each other and a third axis, $\vec{c}$, perpendicular to the plane formed by the first two. Wyckoff (8) generated the atomic position coordinates in terms of these axes using fractions of the unit cell.

Si1: $(\bar{u}, \bar{u}, 1/3)$	Si2: $(u, 0, 0)$	Si3: $(0, u, 2/3)$
O1: (x, y, z)	O2: $(y-x, \bar{x}, z+1/3)$	O3: $(\bar{y}, x-y, z+2/3)$
O4: $(x-y, \bar{y}, \bar{z})$	O5: $(y, x, 2/3-z)$	O6: $(\bar{x}, y-x, 1/3-z)$

The parameters x, y, z and u were evaluated at room temperature by Lepage and Donnay (9) and were reported as:

$$x = 0.41372 \text{ Å} \qquad y = 0.26769 \text{ Å}$$
$$z = 0.11880 \text{ Å} \qquad u = 0.46981 \text{ Å}$$

4

With these parameters, a table of atomic positions for right-hand

α-quartz was constructed (Table I). The nomenclature for the positioning

labels follows that of Nuttal (10).

It is necessary that in order to model a large collection of atoms

with a relatively small cluster, all of the atoms must behave as they

would if located in the larger collection of atoms, regardless of their

position. To accommodate this requirement, the outermost atoms in the

cluster were bonded to hydrogens placed in the proper bond direction,

but at a distance so as to minimize the orbital energy in that direction.

A table of the atomic positions of the replacement hydrogens is included

(Table II). The bond length between oxygens and hydrogens is minimized

to 0.96 $\overset{o}{A}$ (11) whereas the silicon to hydrogen bondlength is 1.48 $\overset{o}{A}$

(12).

Gaussian 80 requires that the cluster be entered into the program

by a means other than the listed atomic positions. The methodology em-

ployed is one of inputting lengths between atoms, and supplying the

angles and dihedral angles between specific groups of atoms. It was

therefore obligatory that a small program be written to provide this

data (Appendix A). These parameters would be varied during the energy

optimization rather than some ubiquitious atomic position.

Gaussian 80

Gaussian 80 (13) is designed to perform ab initio molecular orbital

calculations within the linear combination of atomic orbital framework.

It is an improvement of two earlier, more limited programs, Gaussian 70

and Gaussian 76 (14, 15). Gaussian 80 was originally written for the

DEC VAX-11/780. The IBM version in use for this study was translated

TABLE I

ATOM POSITIONS IN α-QUARTZ AT 300K (in Å)

Atom	x	y	z
Si(0)	0.00000	0.00000	0.00000
O(1,0)	-0.93362	-1.13958	-0.64226
O(2,0)	-0.93362	1.13958	0.64226
O(3,0)	0.93149	0.62166	-1.15981
O(4,0)	0.93149	-0.62166	1.15981
Si(1)	-1.00630	-2.25710	-1.80210
Si(2)	-1.00630	2.25710	1.80210
Si(3)	1.45157	2.00004	-1.80210
Si(4)	1.45157	-2.00004	1.80210
O(1,5)	-1.52635	-3.63545	-1.15981
O(1,6)	-2.01038	-1.76125	-2.96187
O(1,7)	0.44747	-2.49586	-2.44432
O(2,8)	-2.01038	1.76125	2.96187
O(2,9)	0.44747	2.49586	2.44432
O(2,10)	-1.52635	3.63545	1.15981
O(3,11)	2.90532	1.76125	-2.44432
O(3,12)	1.52423	3.11753	-0.64226
O(3,13)	0.44747	2.49586	-2.96187
O(4,14)	0.44747	-2.49586	2.96187
O(4,15)	2.90532	-1.76125	2.44432
O(4,16)	1.52423	-3.11753	0.64226
Si(5)	-2.45780	-4.25712	0.00000
Si(6)	-3.46412	-2.00004	-3.60413
Si(7)	1.45157	-2.00004	-3.60413
Si(8)	-3.46412	2.00004	3.60413
Si(9)	1.45157	2.00004	3.60413
Si(10)	-2.45780	4.25712	0.00000
Si(11)	3.90943	2.25708	-3.60413
Si(12)	2.45789	4.25712	0.00000

TABLE I (Continued)

Atom	x	y	z
Si(13)	-1.00627	2.25708	-3.60413
Si(14)	-1.00627	-2.25708	3.60413
Si(15)	3.90943	-2.25708	3.60413
Si(16)	2.45789	-4.25712	0.00000

TABLE II

HYDROGEN REPLACEMENT POSITIONS (in $\overset{o}{A}$)

Atom	x	y	z
H(0)	0.00000	0.00000	0.00000
H(1,0)	-0.85978	-1.04952	-0.59146
H(2,0)	-0.85978	1.04952	0.59146
H(3,0)	0.85509	0.57067	-1.06469
H(4,0)	0.85509	-0.57067	1.06469
H(1)	-0.97690	-1.80500	-1.33288
H(2)	-0.97690	1.80500	1.33288
H(3)	1.24215	1.44501	-1.54347
H(4)	1.24215	-1.44501	1.54347
H(1,5)	-1.48521	-3.52642	-1.21061
H(1,6)	-1.92806	-1.80190	-2.86679
H(1,7)	0.33246	-2.47697	-2.39351
H(2,8)	-1.92806	1.80190	2.86679
H(2,9)	0.33246	2.47697	2.39351
H(2,10)	-1.48521	3.52642	1.21061
H(3,11)	2.79033	1.78014	-2.39352
H(3,12)	1.51827	3.02587	-0.73739
H(3,13)	0.52979	2.45521	-2.86678
H(4,14)	0.52979	-2.45521	2.86678
H(4,15)	2.79033	-1.78014	2.39352
H(4,16)	1.51827	-3.02587	0.73739
H(5)	-2.08099	-4.00563	-0.46920
H(6)	-2.87875	-1.90389	-3.34552
H(7)	1.04537	-2.20062	-3.13494
H(8)	-2.87875	1.90389	3.34552
H(9)	1.04537	2.20062	3.13494
H(10)	-2.08099	4.00563	0.46920
H(11)	3.50322	2.05649	-3.13493
H(12)	2.08194	3.79825	-0.25861

TABLE II (Continued)

Atom	x	y	z
H(13)	-0.42090	2.35323	-3.34552
H(14)	-0.42090	-2.35323	3.34552
H(15)	3.50322	-2.05649	3.13493
H(16)	2.08194	-3.79825	0.25861

for the AMDAL V7B with IBM's operating system MVS-3.8 by P. N. van Kam-
pen et al. (16).

Gaussian 80 provides programs for the calculation of the one- and
two-electron integers using basis sets of s, p, or d cartesian gaussian
functions. This is the crux of the program and the main point of diver-
gence from other computational programs. Gaussian 80 utilizes a user-
determined number of gaussian functions to reproduce the Slater-type
orbital. These functions can be provided by either the user or the pro-
gram itself. The use of gaussians greatly enhances the speed of the
calculation of the one- and two-electron integrals with little or no
sacrifice of accuracy (17, 18). Moreover, the calculation of the three-
and four-center integrals, which are necessary for clusters of the size
used in this study, are readily handled. Without the Gaussian approxi-
mation, the computing of these integrals proves to be so cumbersome that
it becomes impractical to use them. The one-electron integrals include
the overlap, the kinetic, and the core-Hamiltonian integrals, the x-, y-
and z-dipole integrals, and the one-electron pseudo-potential integral.
The two-electron integral routines included are written for s-, p-, d-
and f-type functions.

After the calculation of these integrals, the programs for the de-
termination of the Hartree-Fock single determinant wave functions and
their associated total energies are initiated. Differing methods are
employed to assess these functions depending on the state of the cluster.
For singlet closed shell states the restricted Hartree-Fock form of the
Roothaan self-consistent-field procedure of repeated diagonalizations
(19) is used. In the case of open-shell states the unrestricted Har-
tree-Fock or the restricted open shell Hartree-Fock methods are used to

obtain the wave functions and energies. Here solutions to the Pople-Nesbet equations (20) or the Binkley-Pople-Dobosh equations (21) respectively are solved through repeated diagonalizations. In each case, the solutions provide detailed information on the orbital interactions and energy levels.

From this point the Mulliken population analysis (22) on the wavefunction is engaged. The dipole moments, including the x-, y- and z-components, of the Hartree-Fock wavefunction are likewise calculated. If the system is open-shelled, the Fermi contact terms and the spin densities for each nucleus are also computed.

Minimum energy optimizations can be performed next. Three methods can be utilized. The simplest of these is the Berney method for geometry optimization. Fletcher-Powell optimization and Murtaugh-Sargent optimization are available as well. These options can be used to map out the stationary points on the potential surfaces as well as locate the energy minimizations.

A number of severe limitations exist in the Gaussian 80 program. The primary constraint lies with the supplied basis set functions. The program provides basis set data for atoms up through the third row of the periodic table. When greater detail on the orbital functions is required, the larger basis sets necessary for the examination are available for only the first and second row atoms. The overall number of basis functions also proved to be limiting. For unrestricted Hartree-Fock calculations, the maximum number of basis functions was 75. With each silicon having nine basis functions, each oxygen five and each hydrogen one, the largest reasonable cluster usable was $Si_3O_8H_8$. As will be seen, this is also the minimal cluster size for this problem. The total

number of primitive gaussians, that is the number of basis functions multiplied by however many gaussians per Slater-Type Orbital (STO) was likewise limited to 361. This imposed a restriction of just four or five gaussian functions per STO, depending on the cluster size. It should be noted, however, that above four gaussians per STO the overall improvement in the results is marginal (17, 18). Lastly, due apparently to the relatively large cluster size, attempts at programmed energy optimization were unsuccessful.

For the purposes of this study only single point runs were done. Basis sets with either three or four gaussians per orbital were used. Most calculations were performed using the smaller basis set, while the larger set was used to examine in detail certain aspects of the calculation. The self-consistent-field calculations were performed using the restricted Hartree-Fock method for the perfect clusters and the unrestricted Hartree-Fock Method for the defects. The output to be utilized included the total electronic energy and the molecular orbital contributions. A full Mulliken population analysis was also obtained. The gross orbital charges and total charge for each atom were calculated as well. The atomic spin densities were generated and the dipole moment was likewise computed. Lastly the Fermi contact analysis was produced. Each feature of this output will be discussed below.

The average running time for the large cluster calculation was approximately 20 minutes. These times varied with cluster size and choice of the number of Gaussians per Slater-Type Orbital. This time also depended on how quickly the electronic energy criterion was met. The average processor storage time, which changed with these considerations as well, ranged from 1.5 to 3.0 M-byte hours. The major contri-

bution to this storage time was made by the 1.2 to 2.0 million integrals calculated in this program.

CHAPTER III

TESTING PROGRAMS

In order to evaluate the ability of the cluster and the program to yield results that simulate the states of the electrons in the infinite crystal, it was necessary to find some means of testing the output from our version of Gaussian 80. This was done in a two-fold manner. First the results for the perfect crystal cluster was considered. Once satisfied that the findings were acceptable, the program was tested by modeling an E_1' center and those results were compared to earlier works and experiments.

The problem of selecting a reasonable model for the perfect crystal proved to be less than straightforward. Because of the aforementioned limitations in basis function and primitive gaussian numbers, it was necessary to use a cluster that was smaller than would otherwise be desired. Working with the assumption that the larger clusters would better simulate the crystal, a tradeoff had to be made between size and accuracy. The two clusters settled upon for the test were the 15-atom $Si_2O_7H_6$ for comparison with Yip's Si_2O_7 and the 21-atom $Si_3O_{10}H_8$ to be used for the E'' center study (Figure 1). As can be seen in the figure, this cluster is also the smallest reasonable cluster for treating the anion divacancy. If the cluster was terminated by $(SiH_3)^+$ rather than $(OH)^-$ radicals, the charges build up unnaturally on the outer silicons and the cluster fails to accurately represent the infinite ideal crystal.
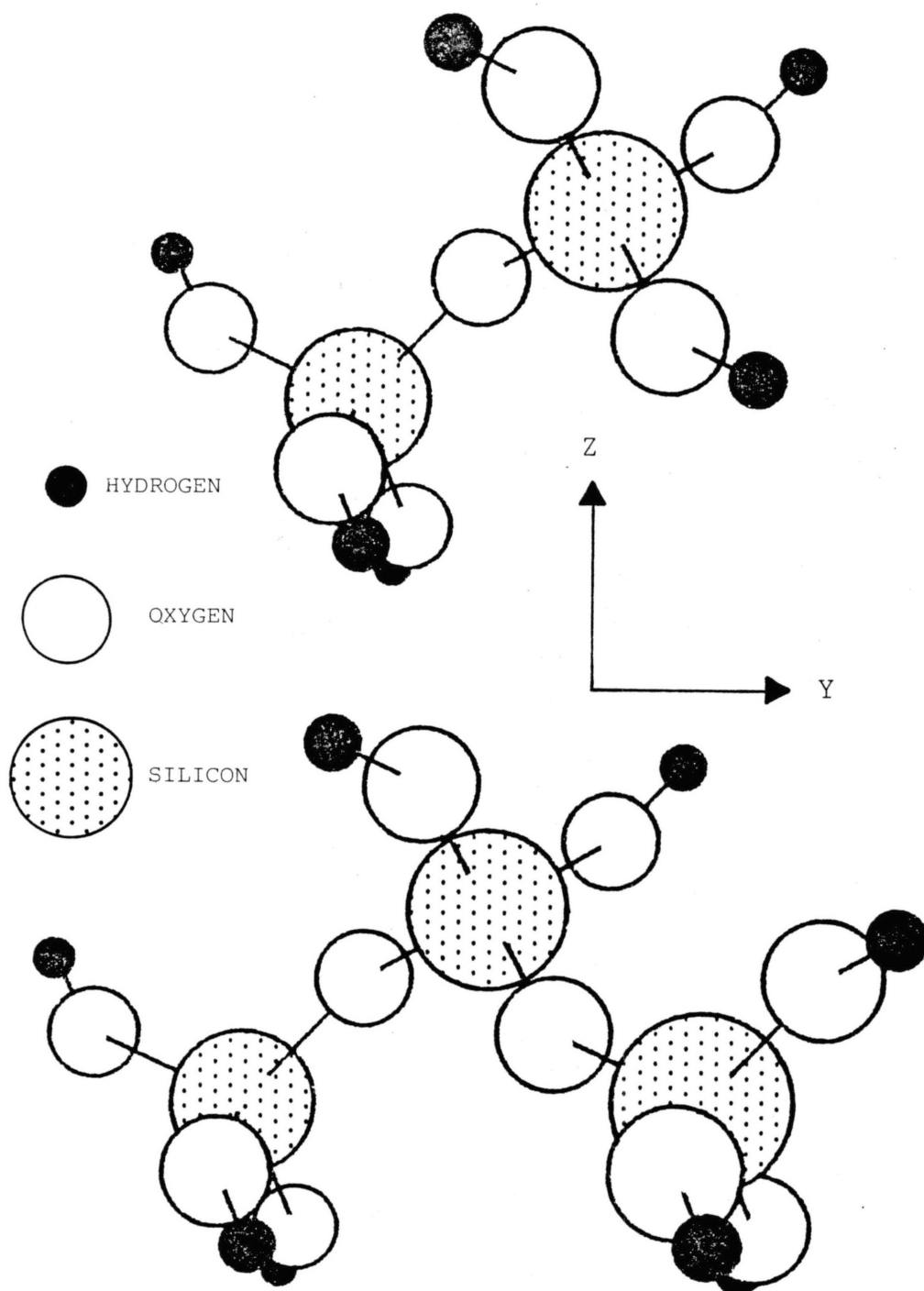
14

HYDROGEN

OXYGEN

SILICON

Z

Y

Figure 1. 15-atom and 21-atom Perfect Clusters

The energy levels for the 15- and 21-atom tests are shown in Figure 2. Listed on the figure are the orbitals which are strongest in each major energy level division. As with Yip, a constant energy value was added appropriately to each reading so as to bring the non-bonding oxygen 2p orbitals to the same energy level. The inner core energy levels are not listed as they fail to interact greatly with the other orbitals and remain fairly constant. Indeed the greatest difference in these inner core levels is but 0.12 eV. The energy levels for the two clusters are compared to the results obtained by Yip and to the electron states calculated by Chelikowsky and Schlüter. It can be seen that the output agrees quite well with that of Chelikowsky's in both magnitude and form. The band structure used for comparison was that at the point M in the first Brillouin zone, the face parallel to the c-axis. This point was selected because it exhibited all of the general behaviors of the other points and because it has relatively low symmetry. The band gap between the bonding oxygen 2p orbitals and the oxygen 2s orbitals is 12.9 eV and 12.7 eV for $Si_2O_7H_6$ and $Si_3O_{10}H_8$ respectively. Chelikowsky calculates this value as 13.2 eV though it drops to as little as 12.3 eV at point A, the center of the face perpendicular to the c-axis. For Yip's Si_2O_7 cluster this gap is 11.7 eV. As the energy levels increase all four results are in broad agreement. There are several small gaps within the bonding oxygen 2p band, the size of which are fairly consistent among the four. In the next band gap, however, there is notable discrepency. The energy difference between the bonding and the non-bonding oxygen 2p orbitals is roughly 1.0 eV in Yip's calculations. In the $Si_2O_7H_6$ and the $Si_3O_{10}H_8$ clusters this difference is 3.5 eV and 3.2 eV. Chelikowsky's
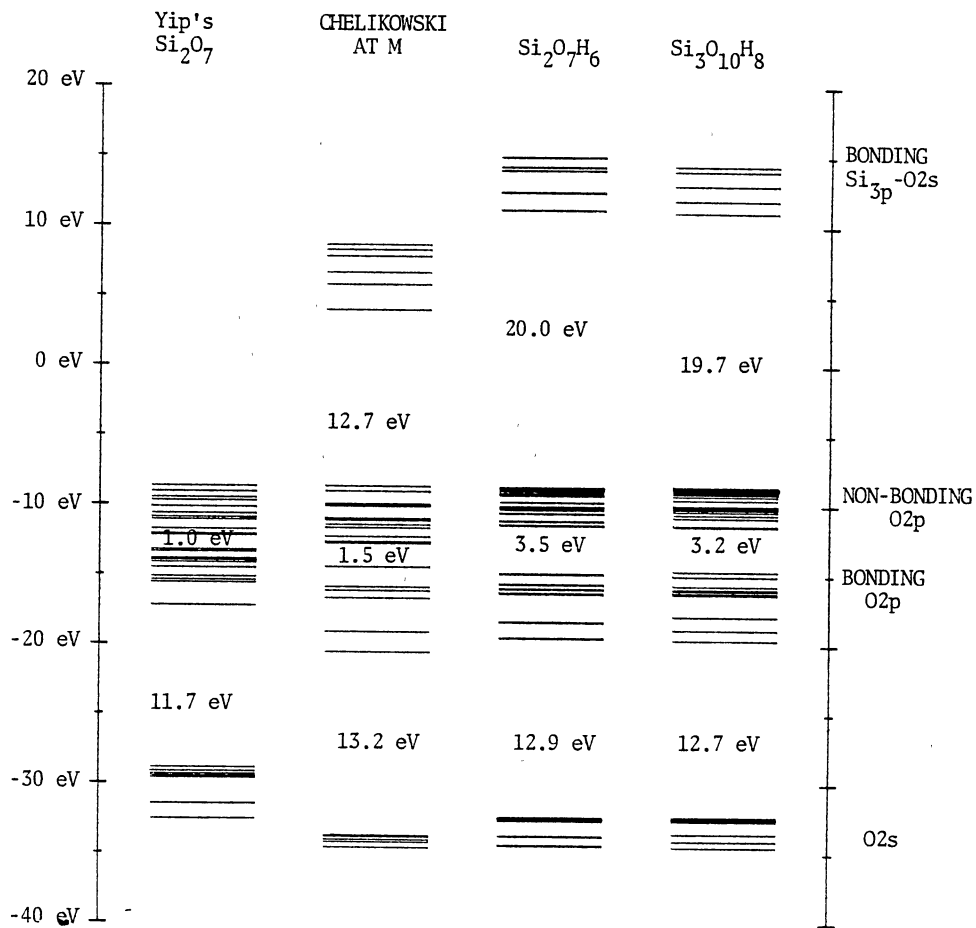
Figure 2. Electron Orbital Energy Levels From
Several Sources

results lie between these sets of values, going from a minimum of 1.5 eV at point M to a maximum of 2.7 eV near Γ, the center of the Brillouin zone. The next large band gap is between the occupied orbitals and the virtual orbitals. Care should be taken when comparing these gaps. The conduction band states in Chelikowsky's results were obtained using a pseudo-potential method. These results are very close to experiment. The method employed in the present study should cause this gap to be too large due to incomplete cancellation of the self-interaction terms in the virtual orbital states. This is, in fact, the case. The gaps for $Si_2O_7H_6$ and $Si_3O_{10}H_8$ are 20.0 eV and 19.7 eV respectively. Chelikowsky shows this gap as 12.7 eV at M. Yip fails to list energy values for orbitals at this level. These results for the perfect cluster indicate that the Gaussian 80 program either match or improve the results obtained by Yip.

Satisfied with the success of the perfect cluster, the E_1' defect test was initiated. This was done by removing the central oxygen in the $Si_2O_7H_6$ cluster leaving one electron in its place, thus allowing the defect to assume a charge of +1. The resulting shift in electronic energy levels is shown in Figure 3, along with the results of Yip's corresponding calculations. In both cases the lowering of energy levels is fairly standard. Yip's calculations exhibit a drop of roughly 6 eV while the present calculation shows a drop averaging 5 eV. There is, however, a notable difference in the behavior of the band gaps. The present work shows a decrease in the energy separation between the oxygen 2s orbitals and the bonding oxygen 2p orbitals from 12.9 eV to 12.6 eV. Yip's results showed a marked increase of over 2.5 eV for this same gap, from 11.7 eV to 14.3 eV. The same is true for the band gap between the bonding and non-bonding
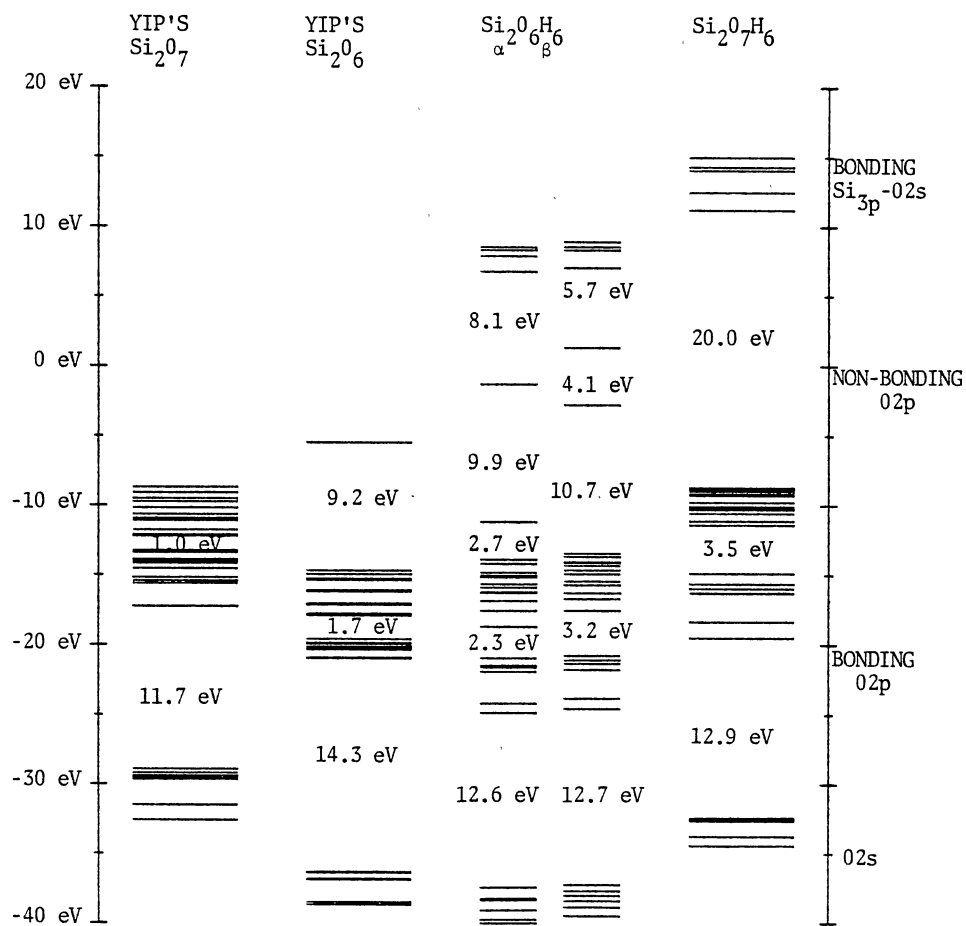
Figure 3. Electron Energy Orbital Levels for the
Perfect Cluster and E'_1-Center Models

oxygen 2p orbitals. In the present calculation this gap decreases from 3.5 eV to 2.3 eV. Yip's work indicates an increase from 1.0 eV to 1.7 eV. Aside from such specific behavior, however, the results of the two calculations show strong similarities with respect to the electronic energy levels. Experimentally, such results have limited applicability. What needs to be addressed are properties of physical significance, the hyperfine tensor and charge distribution.

The charge distribution for the $Si_2O_7H_6$ cluster is shown in Table III. As would be the case in an ideal crystal, the charges are evenly distributed to each atom according to type. Though in distinctly different surroundings, the central oxygen atom has a charge remarkably close to that of the other, outer oxygen atoms, the largest difference being .12 charge units. With the oxygen vacancy, i.e., the E_1' defect, the charge remains fairly well distributed. Alone this lacks meaning but in conjunction with the Fermi contact analysis, the behavior of the defect becomes clear. An examination of this contact analysis (Table III) permits insight to the hyperfine tensor. It should be noted that the actual values for these terms are not exact. No optimizations on atomic positions were performed. The purpose of this test was to verify trends in the E_1' cluster and not to replicate earlier works. Still, the relative values in this analysis are very useful. What can be seen from these results is that the spin density is clearly greater on the short-bond silicon than on the long-bond one, 5.6 times greater. This is just what is found experimentally (22), and again agrees with Yip (5).

The results of these tests show that the Gaussian 80 program can describe α-quartz and the E_1' defect to a degree of accuracy either equal

TABLE III

CHARGE DISTRIBUTION AND FERMI CONTACT TERMS FOR THE 15-ATOM
PERFECT CLUSTER AND E_1' MODEL

Atom	Perfect Cluster Charge	E_1'-defect Cluster Charge	Fermi Contact Terms
O(1,0)	8.707230	-	-
Si(0)	12.483802	12.784060	0.227547
Si(1)	12.475976	12.711954	0.040442
O(2,0)	8.589983	8.559498	0.052888
O(3,0)	8.593221	8.541028	0.093977
O(4,0)	8.592840	8.470092	0.019871
O(1,5)	8.588554	8.497523	0.052152
O(1,6)	8.591984	8.493885	0.012099
O(1,7)	8.593054	8.531179	0.026519
H(2)	0.797427	0.746031	0.006035
H(3)	0.799798	0.746268	0.004884
H(4)	0.801380	0.736629	-0.007596
H(5)	0.787218	0.718118	-0.002724
H(6)	0.795755	0.727521	-0.003744
H(7)	0.801778	0.736214	-0.000076

to or better than previous methods. The answers provided by this program agree both with earlier calculations and experimental observations. Such success lend credence to any findings on the E" center models using Gaussian 80.

CHAPTER IV

EXPERIMENTAL RESULTS

The models selected for studying the E'' centers are shown in Figure 4. Several notable features exist which make this cluster attractive for this project. As stated earlier, the maximum number of basis sets allowable for unrestricted Hartree-Fock calculations was 75. This is exactly the number of basis sets in this divacancy model. For the perfect cluster where only restricted Hartree-Fock calculations are necessary, in which case the limiting number of basis sets is 127, the number of sets is 85. This allows the use of up to four gaussians per Slater-Type Orbital, thus increasing the relative accuracy of the computation. Care was taken to insure that the perfect cluster accurately duplicated the perfect crystal. The net charge on the perfect cluster was therefore maintained to be zero, as it would be in an actual crystal. The charge distributions on the three silicons, though in distinctly differing environs, proved to be surprisingly close. The maximum charge difference between any two silicons was a mere 0.03 charge units. It is clear that even with this limited cluster, a good comparison with experiment should be possible.

Another important feature of this cluster is that it takes on four different forms depending on whether the oxygen vacancies occur in the short-bond or long-bond oxygen atoms. For the purposes of this work the two slightly inequivalent short-bond, long-bond divacancy combinations

Short-bond,
Short-bond
Form

Z

Y

Short-bond,
Long-bond
Form

Long-bond,
Long-bond
Form

● HYDROGEN

○ OXYGEN

⊙ SILICON
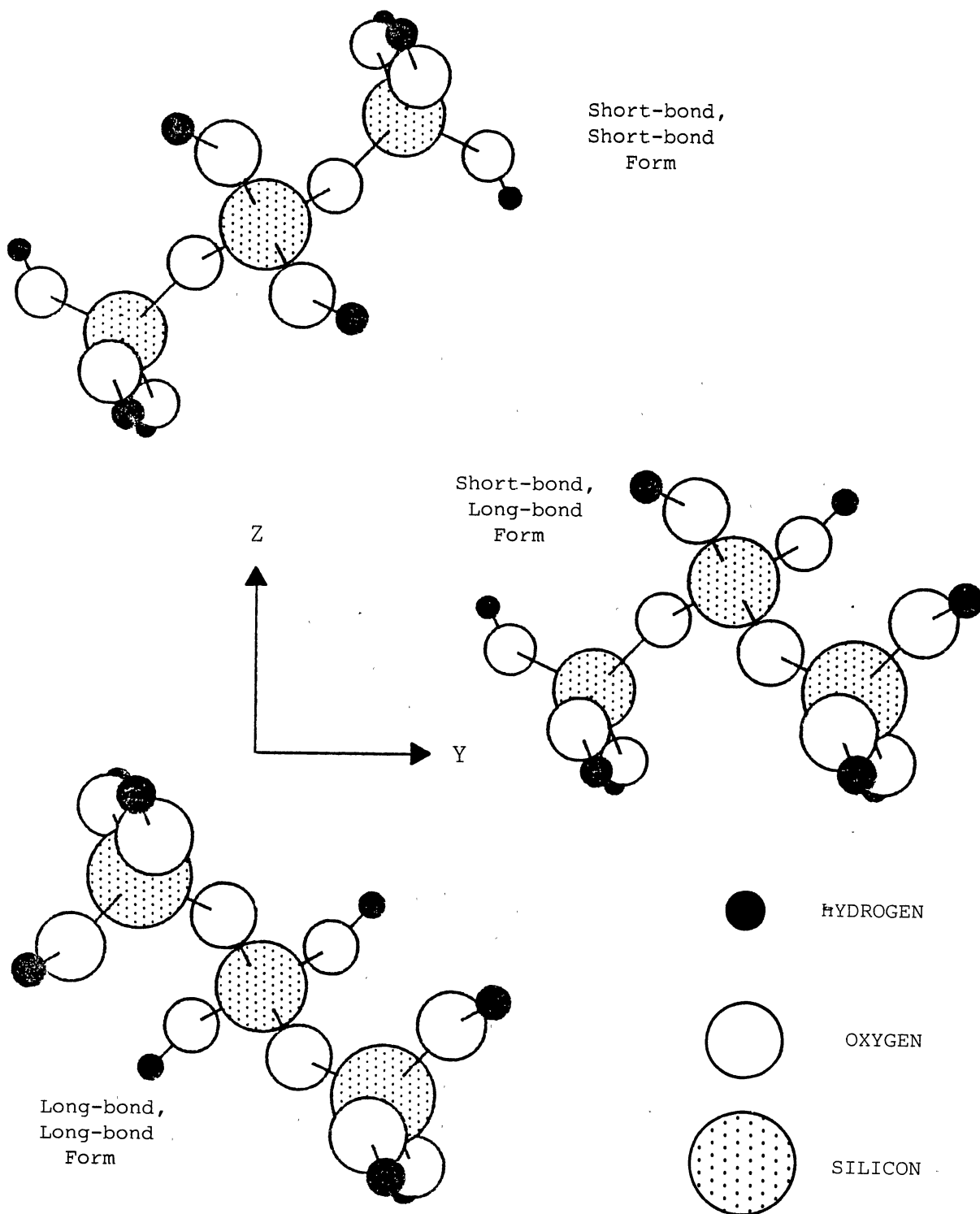
Figure 4. Three Forms of the 21-atom Perfect Cluster

will be taken to be the same. With this, a tentative correlation can be made between the three E'' centers and the three different forms of the cluster. The E'' model is formed by removing the oxygens interjacent to the silicon atoms. In their place two electrons each are allowed. Therefore, unlike a pair of E_1' defects which would have a net charge of +2, the oxygen divacancy model remains uncharged. These unpaired electrons provide the means for several possible silicon interactions; it can assume a spin = 0 or a spin = 1. Each of these states will be studied.

The electron energy levels for the three perfect 21-atom clusters and the smaller 15-atom cluster are illustrated in Figure 5. As can be seen in the diagram, no striking differences exist between the three large clusters. The bonding and non-bonding oxygen orbitals are clearly defined and well separated. In this respect, the three are very similar to the smaller cluster. In detail, however, each of the three forms of the 21-atom cluster have characteristic differences. While it need not be necessary to explore these distinctive features, it is worth noting the semblence of the short-bond, short-bond form and the long-bond, long-bond form.

When the divacancy is formed, two distinct states exist. The un-paired electrons of spin = ½ can interact to form spin = 0 or spin = 1 states. For the spin = 1 case, two spins exist, the α- and β- (or up and down) spins. Figures 6, 7 and 8 show the electronic orbital energy levels for the perfect cluster, the spin = 0 divacancy and the spin = 1 divacancy, α- and β-states of each of the three forms of the cluster. Again, a detailed examination of these energy shifts will not be under-taken as it is beyond the scope of this treatise.

20 eV

10 eV

0 eV

-10 eV

-20 eV

-30 eV

-40 eV

$Si_2O_7H_6$

$Si_3O_{10}H_8$
SHORT-BOND,
SHORT-BOND

$Si_3O_{10}H_8$
SHORT-BOND,
LONG-BOND

$Si_3O_{10}H_8$
LONG-BOND,
LONG-BOND

BONDING
Si_{3p}-O2s

NON-BONDING
O2p

BONDING
O2p

O2s

20.0 eV   19.8 eV   19.7 eV   19.7 eV

3.5 eV   3.0 eV   3.2 eV   3.0 eV

2.1 eV   1.7 eV   1.6 eV   1.7 eV

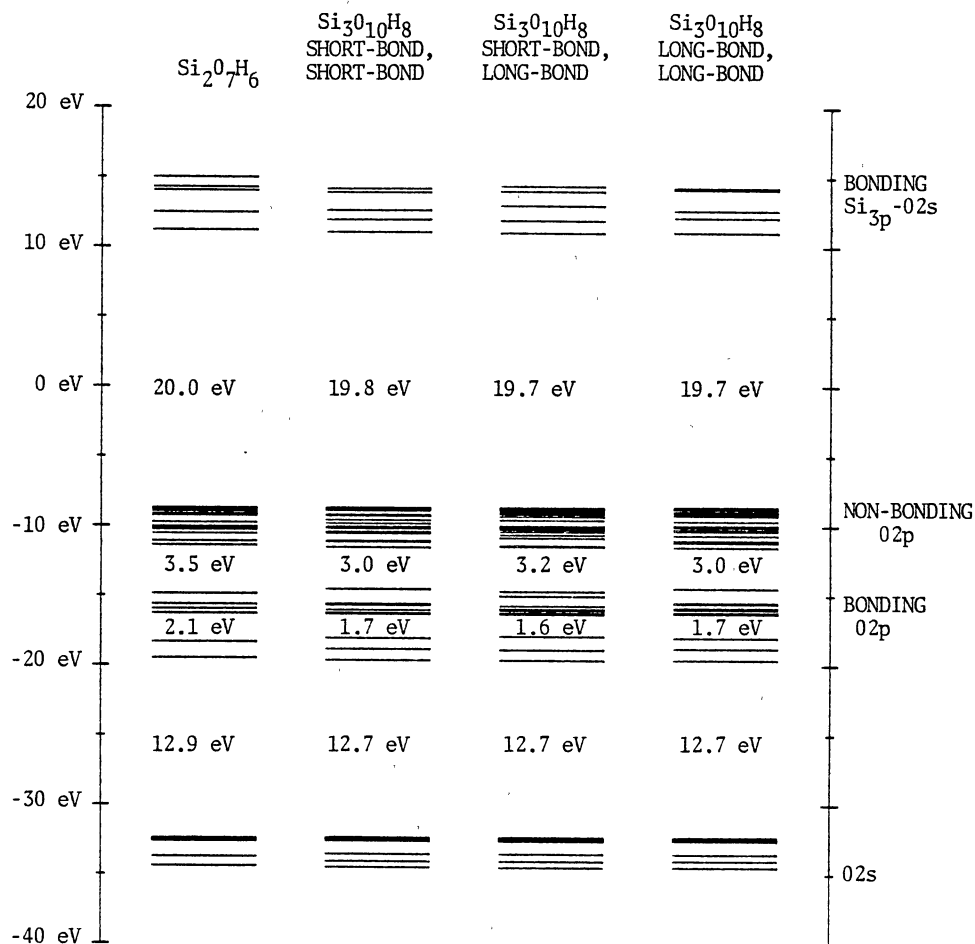12.9 eV   12.7 eV   12.7 eV   12.7 eV

Figure 5.   Electron Orbital Energy Levels for the
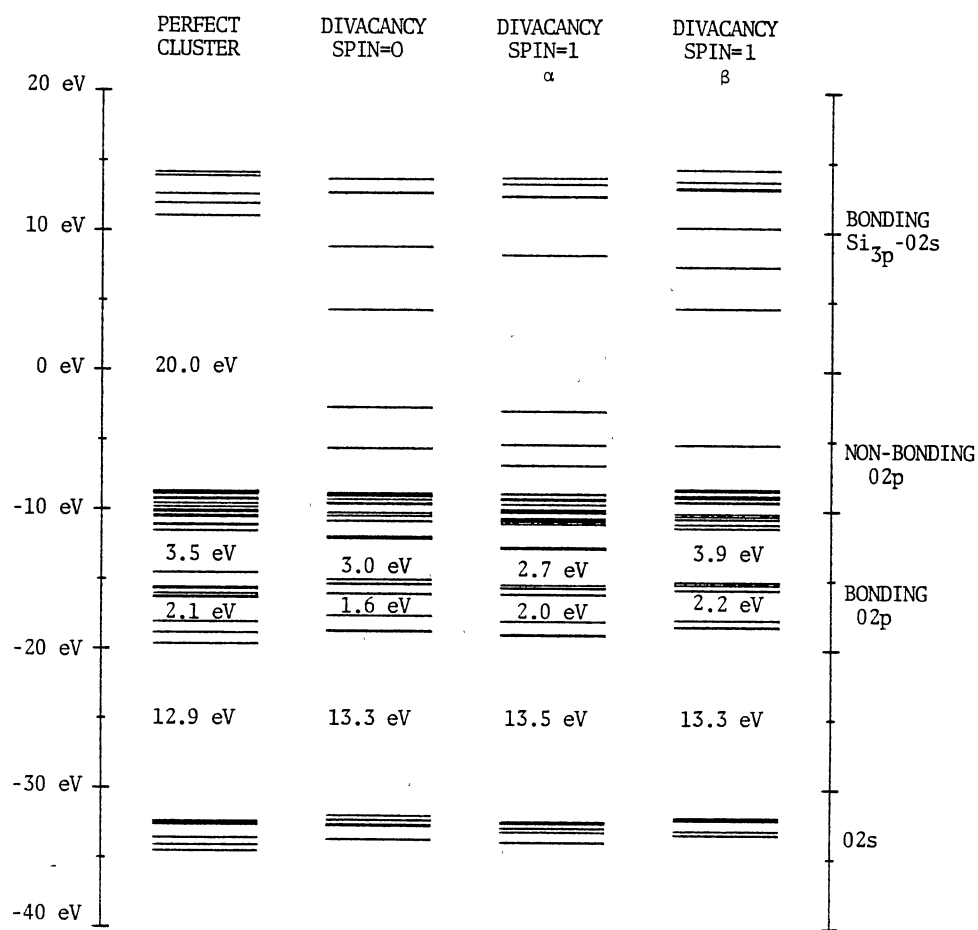15-Atom and Three 21-Atom Perfect
Clusters

Figure 6. Electron Orbital Energy Levels for the
Short-Bond, Short-Bond Cluster
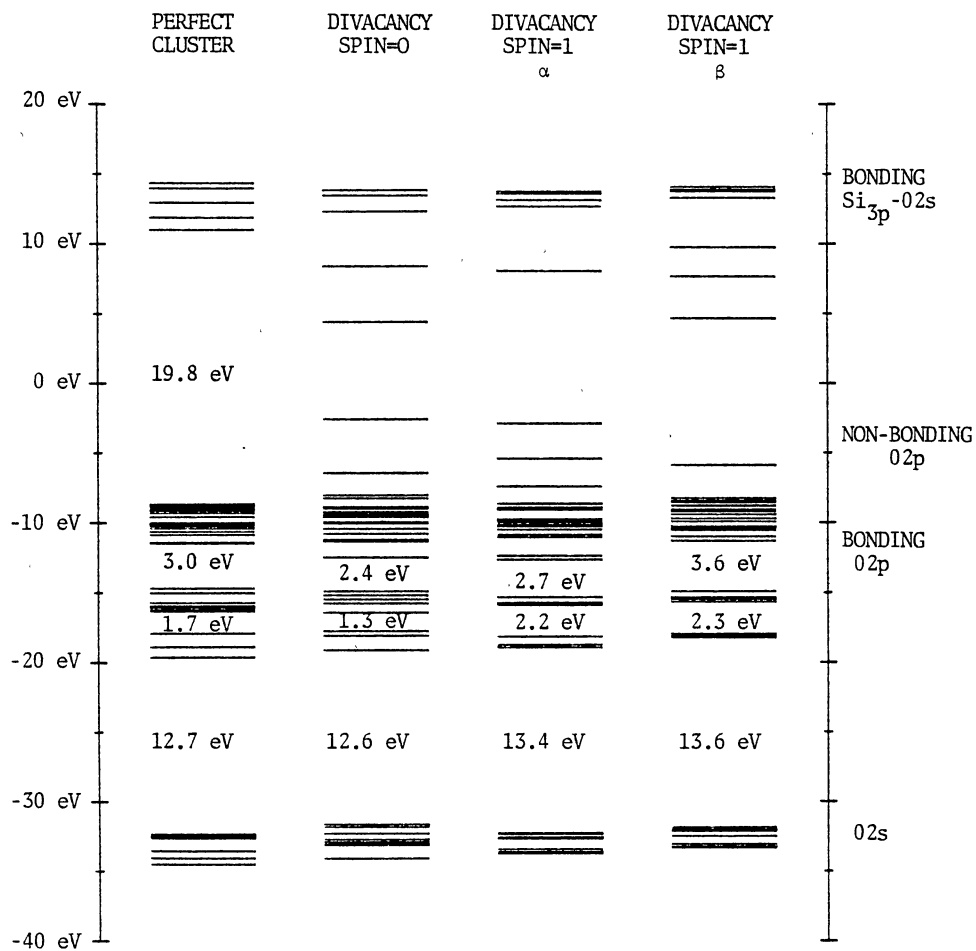
Figure 7. Electron Orbital Energy Levels for the
Short-Bond, Long-Bond Cluster
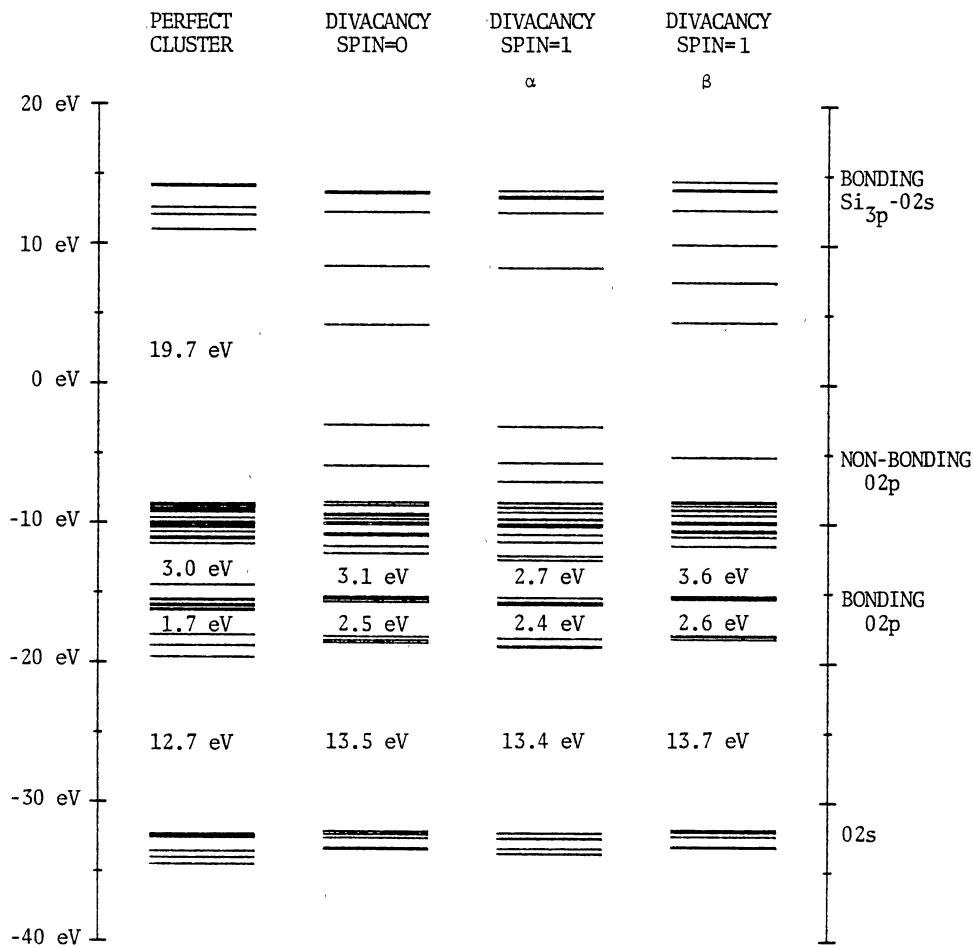
Figure 8. Electron Orbital Energy Levels for the
Long-Bond, Long-Bond Cluster

As in the case with the smaller cluster, the closest tie with experiment is found in the data concerning the charge distribution and spin densities. This information is listed for each atom in each of the three clusters in Tables IV, V and VI. In each of these cases, the perfect clusters exhibit the same charge distribution. The silicons have a charge of approximately +1.5, the interjacent oxygens have a charge roughly -0.7, while the other oxygens have a charge of -0.6. With the divacancy in its place, the central silicon gains some of the electron charge to become +0.7, while the outer silicons obtain a charge of +1.1, i.e., the central silicon is less positive than the outer silicons in both the spin = 0 and spin = 1 cases. The spin densities, however, are much greater on the outer silicons, greater by factor of 3.5 to 5, with the short-bond, long-bond form having the smallest increase and the short-bond, short-bond case having the largest.

Total energies also provide important clues to the behavior of the divacancy (Table VII). Several features should be pointed out. The total energies of each of the three perfect clusters agree to within 0.03 eV. However, with the divacancy in place, each form of the cluster assumes different energies. Once again, the actual values are not as meaningful as relative differences in these values. The energy shift from the spin = 1 divacancy to the perfect cluster is approximately 4 keV. Here the characteristics of the three clusters cause slightly different values. The long-bond, long-bond and short-bond, short-bond forms have a shift of more than 0.2 eV over that of the short-bond, long-bond form. The energies for the double E_1' defects have been included for comparison, as have the charge distributions and the Fermi contact analyses (Table VIII). It should be noted that the spin = 0 states

TABLE IV

CHARGE DISTRIBUTION AND FERMI CONTACT TERMS FOR THE 21-ATOM PERFECT
CLUSTER AND E'' MODEL: SHORT-SHORT FORM

Atom	Perfect Cluster Charge	E''-defect Cluster Charge Spin=0	E''-defect Cluster Charge Spin=1	Fermi Contact Terms
Si(0)	12.509957	13.294664	13.268900	0.187666
O(1,0)	8.709763	-	-	-
O(2,0)	8.709766	-	-	-
Si(1)	12.478873	12.864874	12.881955	0.918058
Si(2)	12.478866	12.864850	12.882152	0.916025
O(3,0)	8.594477	8.565681	8.568911	0.010119
O(4,0)	8.594476	8.565681	8.568812	0.009730
O(1,5)	8.592413	8.566148	8.563325	0.063945
O(1,6)	8.593586	8.574049	8.574545	0.111506
O(1,7)	8.588702	8.569531	8.562184	0.120650
O(1,8)	8.593588	8.574052	8.574625	0.111295
O(1,9)	8.588694	8.569513	8.562038	0.121017
O(1,10)	8.592423	8.566166	8.563225	0.064027
H(3)	0.800399	0.815523	0.809731	-0.000218
H(4)	0.800413	0.815532	0.809769	-0.000365
H(5)	0.796396	0.795504	0.798329	-0.004217
H(6)	0.802785	0.808049	0.812600	0.006050
H(7)	0.787616	0.793322	0.794108	0.001965
H(8)	0.802790	0.808051	0.812497	0.006024
H(9)	0.787631	0.793322	0.794105	0.001907
H(10)	0.796384	0.795487	0.798189	-0.004342

TABLE V

CHARGE DISTRIBUTION AND FERMI CONTACT TERMS FOR THE 21-ATOM PERFECT
CLUSTER AND E'' MODEL: SHORT-LONG FORM

Atom	Perfect Cluster Charge	E''-defect Cluster Charge Spin=0	E''-defect Cluster Charge Spin=1	Fermi Contact Terms
Si(0)	12.504718	13.238072	13.246541	0.285357
O(1,0)	8.710390	-	-	-
O(3,0)	8.708897	-	-	-
Si(1)	12.478602	12.836654	12.884506	0.993626
Si(3)	12.483986	12.928271	12.870785	0.979195
O(2,0)	8.590564	8.562209	8.548082	0.040687
O(4,0)	8.594447	8.564156	8.572470	0.017217
O(1,5)	8.591919	8.560703	8.567378	0.074525
O(1,6)	8.594599	8.570506	8.578740	0.120460
O(1,7)	8.588571	8.567718	8.569277	0.105307
O(3,11)	8.590123	8.582243	8.579116	0.151616
O(3,12)	8.592957	8.578378	8.572358	0.156854
O(3,13)	8.593149	8.576353	8.554970	0.044713
H(2)	0.792138	0.801996	0.813220	0.002455
H(4)	0.802673	0.804443	0.813220	-0.000101
H(5)	0.795493	0.789013	0.804416	-0.004247
H(6)	0.801932	0.799713	0.816719	0.006434
H(7)	0.787743	0.788566	0.801673	0.002174
H(11)	0.797321	0.816241	0.811551	0.016543
H(12)	0.799563	0.824507	0.810440	0.012008
H(13)	0.800213	0.810259	0.795034	-0.005274

TABLE VI

CHARGE DISTRIBUTION AND FERMI CONTACT TERMS FOR THE 21-ATOM PERFECT
CLUSTER AND E'' MODEL: LONG-LONG FORM

Atom	Perfect Cluster Charge	E''-defect Cluster Charge Spin=0	E''-defect Cluster Charge Spin=1	Fermi Contact Terms
Si(0)	12.496668	13.211831	13.251873	0.260626
O(3,0)	8.708343	-	-	-
O(4,0)	8.708328	-	-	-
Si(3)	12.484353	12.892665	12.875779	1.003941
Si(4)	12.484349	12.892640	12.875995	0.995291
O(1,0)	8.592568	8.558969	8.567359	0.016699
O(2,0)	8.592551	8.558954	8.567395	0.019468
O(3,11)	8.589907	8.579527	8.578720	0.148820
O(3,12)	8.593388	8.575701	8.572562	0.144844
O(3,13)	8.593081	8.570000	8.556564	0.055862
O(4,14)	8.593096	8.570022	8.557534	0.055162
O(4,15)	8.589917	8.579526	8.578890	0.146807
O(4,16)	8.593400	8.575711	8.572855	0.143227
H(1)	0.790368	0.790903	0.794797	-0.000947
H(2)	0.790406	0.790942	0.794751	-0.000493
H(11)	0.797731	0.806748	0.813135	0.016140
H(12)	0.800201	0.815939	0.812201	0.011562
H(13)	0.801721	0.803621	0.801744	-0.005487
H(14)	0.801704	0.803614	0.802181	-0.005359
H(15)	0.797727	0.806748	0.813071	0.015925
H(16)	0.800193	0.815939	0.822593	0.011463

TABLE VII

TOTAL CLUSTER ENERGIES

	Short-bond, Short-bond Cluster	Short-bond, Long-bond Cluster	Long-bond, Long-bond Cluster
Perfect Cluster Energy (eV)	-43,593.5393	-43,593.5693	-43,593.5693
Divacancy Spin=0 Energy (eV)	-39,559.4131	-39,559.5902	-39,559.4894
Divacancy Spin=1 Energy (eV)	-39,559.8108	-39,560.0833	-39,559.8626
Spin=0 - Spin=1 (eV)	0.3977	0.4931	0.3732
Spin=1 - Perfect (eV)	4,033.7285	4,033.4860	4,033.7067
Double E_1' Spin=1 Energy (eV)	-39,548.8309	-39,548.3696	-39,548.3342
Double E_1' - Spin=1 Divacancy	10.9799	11.7137	11.5284

TABLE VIII

CHARGE DISTRIBUTION AND FERMI CONTACT ANALYSIS FOR THE THREE
DOUBLE E_1' CLUSTERS

Atom	Short-bond, Short-bond Cluster		Short-bond, Long-bond Cluster		Long-bond, Long-bond Cluster	
	Atomic Charge	Contact Terms	Atomic Charge	Contact Terms	Atomic Charge	Contact Terms
Si	13.2025	0.4114	13.1770	0.1060	13.1071	0.3313
O	-	-	-	-	-	-
O	-	-	-	-	-	-
Si	12.9617	-0.0888	12.6428	-0.0612	12.7314	-0.1676
Si	12.9616	-0.0888	12.7896	0.1278	12.7314	-0.1676
O	8.4146	0.0832	8.2394	0.0844	8.4175	0.0511
O	8.4148	0.0832	8.4870	0.1155	8.4170	0.0510
O	8.4723	0.0050	8.4649	0.0019	8.5485	0.0068
O	8.5224	0.0057	8.5182	0.0077	8.5334	0.0319
O	8.4774	0.0373	8.4973	0.0163	8.3999	0.0054
O	8.5224	0.0057	8.5579	0.0417	8.3998	0.0054
O	8.4774	0.0373	8.5397	0.0826	8.5485	0.0068
O	8.4723	0.0051	8.4474	0.0137	8.5334	0.0318
H	0.6941	-0.0056	0.6331	-0.0185	0.6816	-0.0101
H	0.6941	-0.0056	0.6998	0.0039	0.6815	-0.0101
H	0.7092	-0.0033	0.7005	-0.0031	0.7167	0.0014
H	0.7170	-0.0012	0.7067	-0.0001	0.7200	-0.0006
H	0.7001	-0.0039	0.7068	-0.0017	0.6978	-0.0105
H	0.7170	-0.0012	0.7322	0.0050	0.6978	-0.0105
H	0.7001	-0.0039	0.7334	0.0037	0.7166	0.0014
H	0.7092	-0.0033	0.7266	-0.0087	0.7200	-0.0006

consistently have a greater value than the spin = 1 states. Also noticable is the similarity in the energy difference between the two spin states for the long-bond, long-bond form and for the short-bond, short-bond form, while the short-bond, long-bond case is quite different.

A step-wise Berny optimization was performed on the short-bond, short-bond cluster. The outer silicons were moved symmetrically towards or away from the vacated oxygen positions in steps of 0.05 $\overset{o}{A}$. The silicons were constrained to remain in the original bond direction, so the optimization was not altogether complete. The outcome of this optimization, however, describes the direction of relaxation. The lowest energy state was reached when the silicons relaxed towards the vacancies by roughly 10% of their original bond lengths. The resultant drop in total energy was only 0.14 eV. This energy drop occurred throughout the electronic orbital energies as well, with little effect on the overall characteristics of the cluster.

CHAPTER V

DISCUSSION

Any discussion made at this point should be done within the context
of the experimental work done by Bossoli (4) and Jani (23). Utilizing
the results of experiment to verify the legitamacy of the model, the
model can then be used to shed light on the defect. ESR data indicates
that the electron charges lie close to the central silicon, but the spin
densities are greatest on the outer ones. This holds true for the di-
vacancy model as well. Even in the short-bond, short-bond case, where in
a double E_1' center the spin would affix itself near the silicon on the
short-bond side, the divacancy clearly has the spin on the long-bond
atoms. (Tables IV and VIII). Another important correlation between
experiment and the present study is found in the differences in total
energies between the perfect clusters and the spin = 1 divacancies. Ex-
perimentally the three E'' centers anneal out at differing temperatures.
The E_2'' anneals out completely at 67 C, the E_1'' at 104 C and the E_3'' at
108 C. The difference in the E_1'' and E_3'' temperatures is approximately 10
times the difference in the E_2'' and E_3'' temperatures. The same is true
for the energy differences found in Table VII. The ratio there is 11.
With these energies in mind, a tentative correspondence can be made
between the cluster forms and the separate E'' centers with the long-bond,
long-bond form assigned to the E_1'' center, the short-bond, short-bond form
to the E_3'' center, and the short-bond, long-bond form to the E_2'' center.

This brings to bear another point. Throughout the project the behaviors of the long-bond, long-bond cluster and the short-bond, short-bond cluster have been conspicuously similar. This resemblence is also found experimentally. In both decay properties and annealing conditions, the E_1'' and E_3'' centers are in agreement, but the E_2'' defect differs substantially.

An alternate conclusion can be drawn from these results. It should be recognized that the energy differences under consideration are on the order of 0.5 eV or less. These values are uncomfortably near the relative error of the model. The comparisons are also being made without the benefit of energy optimizations. While there is some justification for relating the energies of the three clusters when in common states, any comparisons between states has limited meaning. Attempting to equate singlet and triplet states has a number of pitfalls. Correlation errors for the two states are different, as are the relaxation forces. This alone could account for the results showing the spin = 1 states being of lower energies than the spin = 0 states. From thermal anneal data, the spin = 0 state would appear to be the more stable state. Indeed, even at room temperatures the E'' centers dissappear after several days. With such a margin of error, the three forms of the cluster cannot be rigorously assigned to the three E'' centers. The divacancy shows, however, the proper characteristics of the E'' center so that it would be plausible to assume that it models at least one of the three E'' defects.

These calculations have demonstrated several points. The oxygen divacancy represents a class of as grown neutral defects. This divacancy can exist not only in the charge = +2 form of a double E_1' but also in the uncharged form used in this study. Moreover, the simple divacancy appears

in three, rather distinct forms. This, in conjunction with the fact that the three clusters from spin = 1 states, as do E" centers, provides a plausible argument for assigning the oxygen divacancy model to at least one of the E" defects. The most convincing evidence is found when comparing the spin densities, wherein the experimental hyperfine data and computational contact analysis agree.

Keeping the computational limitations in mind, several areas do demand further study. A less cursory optimization of atomic positions should be undertaken. This should include both bond-length and bond-angle variation. A more flexible basis set should be employed rather than the minimal STO-3G. The valence state orbitals formed in the spin = 1 divacancy as well as the spin-density should be mapped out. It would be reasonable to assume that the valence state orbitals lie in the plane formed by the three silicons. Such information would greatly aid in forming a better understanding of the model and the E" defect.

The next logical extension of the cluster would be to a four silicon chain. This would allow the divacancy to be separated by more than one silicon, and yet still maintain reasonably strong silicon-silicon interactions. The extended divacancies might well account for the other E" centers. An entire class of spin = 1 defects exist that have yet to be studied in detail and the proximity of the divacancies could very well explain the variance of ESR spectrum intensities.

BIBLIOGRAPHY

(1) Weeks, R. A. and M. M. Abraham, Solid State Division Annual Pro-
     gress Report, Oak Ridge National Laboratory, USA, p. 36
     (1964).

(2) Weeks, R. A. and M. M. Abraham, Bull. Am. Phys. Soc. 10, 374
     (1965).

(3) Solnstev, V. P., R. I. Mashkovtsev and M. Ya. Shcherbakov, J.
     Structural Chem. 18, 578 (1977), Transulated From Zhurnal
     Strukturnol Khimii, 18, 729 (1977).

(4) Bossoli, R. B., M. G. Jani and L. E. Halliburton, Solid State
     Communications 44, 213 (1982).

(5) Yip, K. L. and W. B. Fowler, Phys. Rev. B 11, 2327 (1975).

(6) Isoya, J., J. A. Weil and L. E. Halliburton, J. Chem. Phys. 74,
     5436 (1981).

(7) Mombourquette, M. J., J. A. Weil and P. G. Mezey, Unpublished
     Paper (1983).

(8) Wyckoff, R. W. G., Crystal Structures, Second Edition, Vol. 1
     (1963).

(9) Lepage, Y. and G. Donnay, Acta Crysta. B 32, 2456 (1976).

(10) Nuttal, R. H. D., Ph.D. Dissertation, University of Saskatchewan.

(11) Kuchitsu, K. and L. S. Bartell, J. Chem. Phys. 36, 2460 (1962).

(12) Hehre, W. J., R. Ditchfield, R. F. Stewart and J. A. Pople, J.
     Chem. Phys. 52, 2769 (1970).

(13) Binkley, J. S., R. A. Whiteside, R. Krishnan, H. B. Schlegel, R.
     Seeger, D. J. DeFrees and J. A. Pople, QCPE 406, Indiana
     University.

(14) Hehre, W. J., W. A. Lathan, R. Ditchfield, M. D. Newton and J. A.
     Pople, QCPE 236, Indiana University.

(15) Binkley, J. S., R. A. Whiteside, P. C. Hariharan, R. Seeger, J. A.
     Pople, W. J. Hehre and M. D. Newton, QCPE 368, Indiana Uni-
     versity.

40

(16)   Van Kampen, P. N., F. A. A. M. DeLeeuw, G. F. Smits and C. Altona,
       State University of Leiden. Translation of Gaussian 80 From
       DEC Code to IBM Code.

(17)   Hehre, W. J., R. F. Stewart and J. A. Pople, J. Chem. Phys. 51,
       2657 (1969).

(18)   Tatewaki, H., J. Chem. Phys. 74, 4207 (1981).

(19)   Roothaan, C. C. J., Rev. Mod. Phys. 23, 69 (1951).

(20)   Pople, J. A. and R. K. Nesbet, J. Chem. Phys. 22, 571 (1954).

(21)   Binkley, J. S., J. A. Pople and P. A. Dobosh, Mol. Phys. 28, 1423
       (1974).

(22)   Mulliken, R. S., J. Chem. Phys. 23, 1833 (1955).

(23)   Jani, M., G. R. B. Bossoli and L. E. Halliburton, Phys. Rev. B 27,
       2285 (1983).

APPENDIX

CALCULATION OF INTERATOMIC DISTANCES, ANGLES

AND DIHEDRAL ANGLES

```
10   !
20   !          A PROGRAM TO CALCULATE THE INTERATOMIC
30   !          DISTANCES, ANGLES AND DIHEDRAL ANGLES
40   !
50   OPTION BASE 1
60   DIM X(21),Y(21),Z(21),D(21,21)
70   INTEGER A,B,C,D,I,J,K,Imax
80   Imax=21
90   FIXED 4
100 Degrees:   DEG
110  PRINT "  ATOM  ";"    X   ";"    Y   ";"    Z    "
120  FOR I=1 TO Imax
130  READ X(I),Y(I),Z(I)
140  PRINT I;X(I);Y(I);Z(I)
150  NEXT I
160  PRINT
170  PRINT " ATOM(1)";" ATOM(2)";" ATOM(3)";"    ANGLE"
180  !
190  !          CALCULATION OF THE INTERATOMIC DISTANCES
200  !
210  FOR I=1 TO Imax
220  FOR J=1 TO Imax
230  IF J=I THEN 260
240  D(I,J)=SQR((X(I)-X(J))^2+(Y(I)-Y(J))^2+(Z(I)-Z(J))^2)
250  PRINT I;J;D(I,J)
260  NEXT J
270  NEXT I
280  !
290  !          CALCULATION OF THE INTERATOMIC ANGLES
300  !
310  FOR I=1 TO Imax              !   IT IS NOT NECESSARY TO
320  FOR J=1 TO Imax              !   RUN THROUGHOUT ALL
330  FOR K=1 TO Imax              !   POSSIBLE COMBINATIONS.
340  IF I=J THEN GOTO 450         !   Imax SHOULD BE ADJUSTED
350  IF J=K THEN GOTO 440         !   TO FIT THE NEED.
360  IF I=K THEN GOTO 440         !
370  Px=(X(J)-X(I))*(X(J)-X(K))   !
380  Py=(Y(J)-Y(I))*(Y(J)-Y(K))   !   _     _
390  Pz=(Z(J)-Z(I))*(Z(J)-Z(K))   !   A dot B = !A!*!B!*COS(Theta)
400  Pd=D(J,I)*D(J,K)             !
410  Theta=(Px+Py+Pz)/Pd          !
420  T=ACS(Theta)                 !
430  PRINT I;J;K;T                !
440  NEXT K                       !
450  NEXT J
460  NEXT I
470  !
480  !          CALCULATION OF THE DIHEDRAL ANGLES
490  !
500  PRINT
510  PRINT " ATOM(1)";" ATOM(2)";" ATOM(3)";" ATOM(4)";"    DIHED."
520  FOR A=1 TO Imax              !
530  FOR B=1 TO Imax              !
540  FOR C=1 TO Imax              !   AGAIN, THESE SHOULD BE
550  FOR D=1 TO Imax              !   ADJUSTED AS IS NEEDED.
```

```
560   IF A=B THEN GOTO 930            !
570   IF A=C THEN GOTO 920            !
580   IF B=C THEN GOTO 920            !
590   IF A=D THEN GOTO 910            !
600   IF B=D THEN GOTO 910            !
610   IF C=D THEN GOTO 910            !
620   Ax=X(A)-X(B)                    !   TO FIND THE DIHEDRAL
630   Ay=Y(A)-Y(B)                    !   ANGLE BETWEEN ANY FOUR
640   Az=Z(A)-Z(B)                    !   POINTS, THE MIDDLE TWO
650   Cx=X(C)-X(B)                    !   POINTS ARE USED AS AN
660   Cy=Y(C)-Y(B)                    !   AXIS FROM WHICH THE PER-
670   Cz=Z(C)-Z(B)                    !   PENDICULAR PROJECTIONS
680   Axcx=Ay*Cz-Az*Cy               !   OF THE OUTER TWO POINTS
690   Axcy=Az*Cx-Ax*Cz               !   ARE FOUND.  THE LENGTH
700   Axcz=Ax*Cy-Ay*Cx               !   OF THE AXIS IS THEN
710   Bx=X(B)-X(C)                    !   SUBTRACTED AWAY AND THE
720   By=Y(B)-Y(C)                    !   ANGLE BETWEEN THE TWO
730   Bz=Z(B)-Z(C)                    !   PERDENDICULAR PROJECTIONS
740   Dx=X(D)-X(C)                    !   IS FOUND IN THE SAME
750   Dy=Y(D)-Y(C)                    !   MANNER AS ABOVE.
760   Dz=Z(D)-Z(C)                    !
770   Dxbx=Dy*Bz-Dz*By               !
780   Dxby=Dz*Bx-Dx*Bz               !
790   Dxbz=Dx*By-Dy*Bx               !
800   Pxx=Dxbx*Axcx                  !
810   Pyy=Dxby*Axcy                  !
820   Pzz=Dxbz*Axcz                  !
830   Da=SQR(Axcx^2+Axcy^2+Axcz^2)   !
840   Dd=SQR(Dxbx^2+Dxby^2+Dxbz^2)   !
850   Pdd=Da*Dd                       !
860   Phi=(Pxx+Pyy+Pzz)/Pdd          !
870   IF Phi>1 THEN Phi=1            !   THIS MAINTAINS THE
880   IF Phi<-1 THEN Phi=-1         !   DIHEDRAL ANGLE TO BE
890   Dh=180-ACS(Phi)               !   LESS THAN 180 DEGREES
900   PRINT D;C;B;A;Dh
910   NEXT D
920   NEXT C
930   NEXT B
940   NEXT A
950   !
960   !                    ATOMIC POSITIONS
970   !
980   DATA    1.04537,-2.20062,-3.13494
990   DATA   -2.87875,-1.90389,-3.34552
1000  DATA   -2.08099,-4.00563,-0.46920

1170  DATA   -0.93362, 1.13958, 0.64226
1180  DATA    0.00000, 0.00000, 0.00000
1190  STOP
1200  END
```

VITA

Brian Leonard Mihura

Candidate for the Degree of

Master of Science

Thesis: OXYGEN DIVACANCY MODEL FOR THE E" CENTERS IN CRYSTALLINE SiO$_2$

Major Field: Physics

Personal Data: Born in Ft. Worth, Texas, February 28, 1959, the son of Max Lee and Cloan Mihura.

Education: Graduated from Gosnell High School, Gosnell, Arkansas, in 1977. Received Bachelor of Science degree in physics with minor degress in history and german from Oklahoma State University, Stillwater, Oklahoma, in December, 1981; completed requirements for the Master of Science degree at Oklahoma State University in July, 1984.

Experience: Undergraduate and Graduate Teaching and Research Assistant, Oklahoma State University, Stillwater, Oklahoma, 1978-1983.